Journal of the Korean Physical Society, Vol. 53, No. 6, December 2008, pp. 3578∼3583

Influence of Mask Feature on the Diffracted Light in Proximity and Contact Lithography

Sang-Kon KIM* and Hye-Keun OH
Department of Applied Physics, Hanyang University, Ansan 426-791

(Received 21 August 2007)

Simple nanolithography methods, which provide increasing resolution at a fraction of the cost of conventional steppers, are of major interest. Methods, such as nano-imprint lithography, interferometric and laser direct-write techniques and the evanescent near-field optical lithography, are becoming increasingly important. Those low-cost optical contact lithography techniques can produce below 45-nm features by using ultraviolet radiation without a complex optical system.

In this paper, for the usability of the proximity printing applications, diffraction effects are analyzed with the rigorous electromagnetic calculations when the ratio of mask pattern to the incident wavelength is below one. For this purpose, an analytical model and two models of a rigorous coupled-wave analysis are described and analyzed. The simulated results show good agreement with the experimental results. When the ratio of the pitch to the wavelength is small, the transverse electric (TE) and the transverse magnetic (TM) polarizations with the nonspecular (+1 and −1 orders) harmonics are small in comparison to those with the specular (0 order) harmonic and the variance of the TE and the TM polarizations is produced. When the pitch is smaller than incident wavelength, according to the incident angle, the variation in the diffraction efficiency with the 0 order is decreased. The variance of the TE and the TM polarizations and the diffraction efficiency can degrade the resolution of pattern formation for patterns smaller than the incident wavelength.

PACS numbers: 85.40.Hp, 78.40.Fy, 78.20.Bh, 85.40.+j
Keywords: Microlithography, Lithography simulation, Proximity and contact lithography, Mask polarization, Rigorous coupled-wave analysis

I. INTRODUCTION

Pattern reduction has created a great deal of interest in finding effective methods to reduce the feature sizes of microelectronic and data-storage devices [1,2]. This technology can realize the micro / nano systems of integrated functional elements in different domains, such as mechanics, electronics, chemistry, optics and biotechnology, to support a highly-networked information society, an aging society and an eco-friendly society in the 21st century [3]. Hence, simple and cheap nanolithography technologies, which are nano-imprint lithography, interferometric and laser direct-write techniques and evanescent near-field optical lithography, are interesting to reduce the fabrication cost and to produce quickly various micro / nano systems.

In this paper, for the proximity printing applications, when the mask pattern is smaller than an incident wavelength, the diffraction effects of the transverse electric (TE) and the transverse magnetic (TM) polarizations in a mask are analyzed by using an analytical model and rigorous electromagnetic calculations. For the rigorous calculation, the rigorous coupled-wave analysis (RCWA), which is a rigorous and efficient method for calculating the coupled-wave diffraction in periodic gratings of arbitrary thickness without numerical problems, is used [4, 5]. Diffraction effects depend on the pattern shapes of the mask, the pattern size of mask, the material properties and the resist depth. In this simulation, the effects of grating depths and incident angles are calculated in terms of the ratio of pitch to wavelength. Simulation results are compared with experiment results. The reduction method for diffraction effects is a serious topic for improving the resolution of pattern formation.

II. ANALYTICAL MODEL

Figure 1 shows a mask structure in (a) two-dimensions and (c) three-dimensions. Figure 1(b) shows the simplified three regions of a mask. An incident wave enters at the plane of incidence in the top mask and the diffracted waves transmit at the bottom mask in Figure 1(a). When a mask pattern is smaller than an incident wavelength, the effects of diffractive directions can′t be ignored. After light transfers through a mask of a single slit (a dense

*E-mail: sangkona@hotmail.com; http://www.sangkon.info

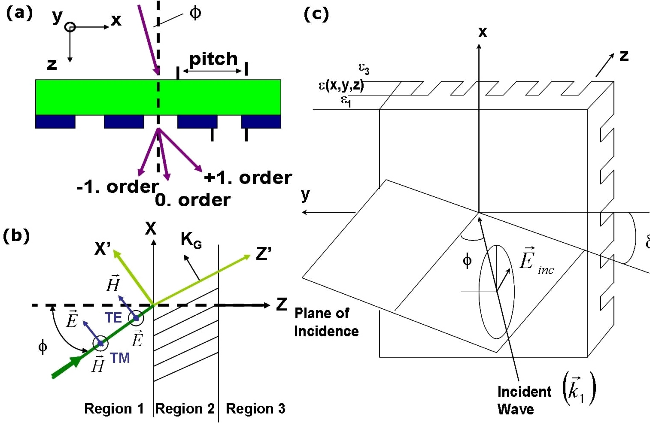

Fig. 1. A mask structure in (a) two-dimensions and in (c) three-dimensions. (b) The simplified three regions of the mask.

slit), the scalar electric field $\mathbf{E}_{Single}$ ($\mathbf{E}_{Dense}$) in the x-direction is

$$\begin{aligned}\mathbf{E}_{Single}(x) &= \sum T_m \exp(i2\pi f_x x) \\ &= \int_{-L/2}^{L/2} e^{i2\pi f_x x} dx = \left[\frac{1}{2\pi i f_x} e^{i2\pi f_x x}\right]_{-L/2}^{L/2} \\ &= \frac{\sin(\pi f_x L)}{\pi f_x},\end{aligned} \quad (1)$$

$$\begin{aligned}\mathbf{E}_{Dense}(x) &= \sum\sum T_m \exp(i2\pi f_x (x + np)) \\ &= \frac{\sin(\pi f_x L)}{\pi f_x} \sum \delta\left(f_x - \frac{n}{p}\right),\end{aligned} \quad (2)$$

where T_m is the transmittance of mask, f_x is a space frequency in the x-direction, L is a slit width, n is a number and p is the pitch of the mask pattern. When the direction of a slit is in the y-direction, the diffraction effects are considered in the x-direction.

For a single slit, the intensities of the x-axis and y-axis polarizations can be assumed to be

$$I_{X-pol}(\sigma_x) = \left[\frac{\sin\left(\pi L \frac{\sigma_x}{\lambda}\right)}{\pi L \frac{\sigma_x}{\lambda}}\right]^2,$$

$$I_{Y-pol}(\sigma_x) = (1 - \sigma_x^2)\left[\frac{\sin\left(\pi L \frac{\sigma_x}{\lambda}\right)}{\pi L \frac{\sigma_x}{\lambda}}\right]^2, \quad (3)$$

where σ_x ($= \lambda f_x$) is the direction cosine. For a dense slit, the intensities of the x-axis and the y-axis polarizations can be assumed to be

$$I_{X-pol}(n) = \left[\frac{\sin\left(\pi L \frac{n}{p}\right)}{\pi L \frac{n}{p}}\right]^2 = \left[\frac{\sin\left(\pi \frac{L}{\lambda}\left(n\frac{\lambda}{p}\right)\right)}{\pi \frac{L}{\lambda}\left(n\frac{\lambda}{p}\right)}\right]^2,$$

$$I_{Y-pol}(n) = \left[1 - \left(n\frac{\lambda}{p}\right)^2\right]\left[\frac{\sin\left(\pi \frac{L}{\lambda}\left(n\frac{\lambda}{p}\right)\right)}{\pi \frac{L}{\lambda}\left(n\frac{\lambda}{p}\right)}\right]^2, \quad (4)$$

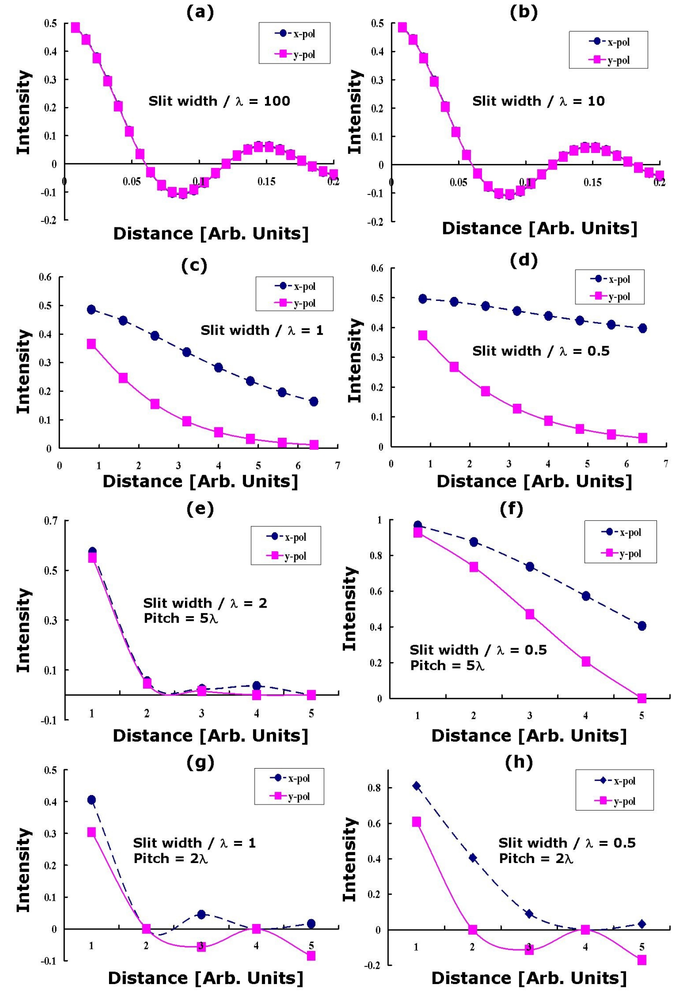

Fig. 2. Effects of the diffractive directions of a single slit with (a) slit width (L) / wavelength (λ) = 100, (b) $L/\lambda = 10$, (c) $L/\lambda = 1$ and (d) $L/\lambda = 0.5$ and of a dense slit with (e) $L/\lambda = 2$ and pitch (p) / wavelength (λ) = 5, (f) $L/\lambda = 0.5$ and $p/\lambda = 5$, (g) $L/\lambda = 1$ and $p/\lambda = 2$ and (h) $L/\lambda = 0.5$ and $p/\lambda = 2$ due to the ratios of a slit width and pitch to wavelength. 'x-pol' and 'y-pol' in the graph legends indicate 'x- polarization' and 'y- polarization', respectively.

when the direction cosine σ_x is $n\lambda/p$ and p is pitch in Figure 1(a).

Figure 2 shows the effects of the diffractive directions in terms of the ratio of the slit width to the wavelength. For the single silt in Figures 2(a) – (d), the difference between the x-polarization and the y-polarization is small when the slit width is larger than the wavelength, but this difference becomes large when the slit width is the same as or smaller than the wavelength. For the dense silt in Figures 2(e) – (h), the difference between the x-polarization and the y-polarization is large when the ratio of the slit width to the incident wavelength and the ratio of the pitch to the incident wavelength are small. When the mask pattern and the pitch are smaller than the wavelength, this difference is larger. Hence, when the

silt width is smaller than the wavelength, the diffraction effects of the x- and the y-polarizations can′t be ignored.

III. RIGOROUS COUPLED WAVE ANALYSIS (RCWA)

A mask structure can be simplified into three regions, which are planes in regions 1 and 3 and an inhomogeneous plane in the grating region 2 in Figure 1(b). Each of the waves in the three regions satisfies Maxwell equations:

$$\nabla \cdot \mathbf{D} = \nabla \cdot (\varepsilon \mathbf{E}) = 0, \nabla \times \mathbf{E} = -\frac{\partial \mathbf{B}}{\partial t} = -\mu_0 \frac{\partial \mathbf{H}}{\partial t}, \quad (5)$$

$$\nabla \cdot \mathbf{H} = 0, \nabla \times \mathbf{H} = \mathbf{j} + \frac{\partial \mathbf{D}}{\partial t} = \sigma \mathbf{E} + \varepsilon \frac{\partial \mathbf{E}}{\partial t}, \quad (6)$$

where $\mathbf{E}\,(\mathbf{B})$ is the electric (magnetic) field, $\mathbf{H}$ is the magnetic intensity, $\mathbf{D}$ is the electric displacement, $\mathbf{j}$ is the current density, μ is the permeability, ε is the permittivity and σ is the conductivity. When the electric field and the magnetic intensity may be expressed as $\mathbf{E} = \mathbf{E}\exp(j\omega t)$ and $\mathbf{H} = \mathbf{H}\exp(j\omega t)$, respectively, the vector diffraction equations can be assumed to be

$$\nabla^2 \mathbf{E} + \nabla\left(\mathbf{E} \cdot \frac{\nabla \varepsilon}{\varepsilon}\right) + \left(\frac{2\pi}{\lambda}\right)^2 \varepsilon \mathbf{E} = 0,$$

$$\nabla^2 \mathbf{H} + \frac{\nabla \varepsilon}{\varepsilon} \times \nabla \times \mathbf{H} + \left(\frac{2\pi}{\lambda}\right)^2 \varepsilon \mathbf{H} = 0, \quad (7)$$

By using $\mathbf{H} = (0, H_y(x,z), 0), \nabla \times (\nabla \times f) = \nabla(\nabla \cdot f) + \nabla \cdot (\nabla f) = 0 + \nabla \cdot (\nabla f)$ and $\frac{\partial}{\partial y} H_y(x,z) = 0$, the TM mode of Eq. (7) can be assumed to be

$$\nabla^2 H_y - \left(\frac{\nabla \varepsilon(x,z)}{\varepsilon(x,z)} \cdot \nabla\right) H_y + \left(\frac{2\pi}{\lambda}\right)^2 \varepsilon(x,z) H_y = 0. \quad (8)$$

By using $\mathbf{E} = (0, E_y(x,z), 0)$, the TE mode of Eq. (7) can be assumed to be

$$\nabla^2 E_y + \left(\frac{2\pi}{\lambda}\right)^2 \varepsilon(x,z) E_y = 0. \quad (9)$$

For the incident light of Figure 1(b), the total electric field of region 1 can be assumed to be

$$E_1 = \exp(-j\mathbf{k_1} \cdot \mathbf{r}) + \sum_{i=-\infty}^{\infty} R_i \exp(-j\mathbf{k_{1,i}} \cdot \mathbf{r}), \quad (10)$$

where $\mathbf{k_1}$ is a wave vector, $\mathbf{r}$ is the distance vector, R_i is the normalized amplitude of the ith reflected wave and $\mathbf{k}_{1,i}$ is a wave vector of the ith reflected wave. The total electric field in region 3 of Figure 1(b) can be assumed to be

$$E_3 = \sum_{i=-\infty}^{\infty} T_i \exp[-j\mathbf{k_{3,i}} \cdot (\mathbf{r} - d\hat{z})], \quad (11)$$

where T_i is the normalized amplitude of the ith transmitted wave in region 3 with the wave vector $\mathbf{k}_{3,i}$. The total electric field in region 2 of Figure 1(b) can be assumed to be

$$E_{2,n} = \sum_{i=-\infty}^{\infty} S_{i,n}(z) \exp(-j\sigma_{i,n} \cdot \mathbf{r}), \quad (12)$$

where i is the space-harmonic index, $S_{i,n}(z)$ is the space-harmonic field amplitude of the nth slab, the wave vector $\sigma_{i,n}$ is $\mathbf{k}_{2,n} - i\mathbf{K}$ and K is the magnitude of the grating vector ($K = 2\pi/\Lambda$, where Λ is the grating period).

The relative permittivity for the nth slab grating in region 2 can be assumed to be

$$\varepsilon_n(x, z_n) = \varepsilon_{III} + (\varepsilon_{III} - \varepsilon_I) \times \sum_{h=-\infty}^{\infty} \tilde{\varepsilon}_{h,n} \exp(jhKx), \quad (13)$$

$$\tilde{\varepsilon}_{h,n} = (1/\Lambda) \int_0^{\Lambda} f(x, z_n) \exp(-jhKx)\, dx, \quad (14)$$

where z_n is the z coordinate of the nth slab, h is the harmonic index and $f(x, z_n)$ is 0 or 1 [6]. Hence, the electromagnetic fields can be described as Floquet expansions of the fields in region 2 and as plane waves of regions 1 and 3 by using the polynomial expansion. For the calculation of the electromagnetic fields and the diffraction efficiencies, the electromagnetic equations of Eqs. (8) and (9) can be solved by using the assumed fields of Eqs. (10)−(14) and the boundary conditions (the continuity of tangential fields).

Another method is to use a scattering matrix. The scattering matrix (S) relates all incoming waves to a port to all outgoing waves from the port. The transmission matrix (T) relates all the waves from the same side of the port to all the waves of the opposite side of the port:

$$\begin{bmatrix} c_0^{(+)} \\ c_0^{(-)} \end{bmatrix} = \begin{bmatrix} T_{00} & T_{01} \\ T_{10} & T_{11} \end{bmatrix} = \begin{bmatrix} c_1^{(+)} \\ c_1^{(-)} \end{bmatrix},$$

$$\begin{bmatrix} c_1^{(+)} \\ c_0^{(-)} \end{bmatrix} = \begin{bmatrix} S_{00} & S_{01} \\ S_{10} & S_{11} \end{bmatrix} = \begin{bmatrix} c_0^{(+)} \\ c_1^{(-)} \end{bmatrix}, \quad (15)$$

where $c_0^{(+)}$ and $c_0^{(-)}$ are the input amplitudes of the incident direction and the reflected direction in the incident plane, respectively and $c_1^{(+)}$ and $c_1^{(-)}$ are the output amplitudes of the reflected direction and the incident direction in the output plane, respectively [7]. For a stack of thin films with n layers, the matrix $T(n, n+1)$ is composed of a propagation matrix (D) and an interface matrix (N):

$$T(n, n+1) = \begin{bmatrix} T_{00}^{n,n+1} & T_{01}^{n,n+1} \\ T_{10}^{n,n+1} & T_{11}^{n,n+1} \end{bmatrix} = \begin{bmatrix} D^{n,n+1} & 0 \\ 0 & \left(D^{n,n+1}\right)^{-1} \end{bmatrix} \begin{bmatrix} N_{00}^{n,n+1} & n_{01}^{n,n+1} \\ N_{10}^{n,n+1} & N_{11}^{n,n+1} \end{bmatrix}, \quad (16)$$

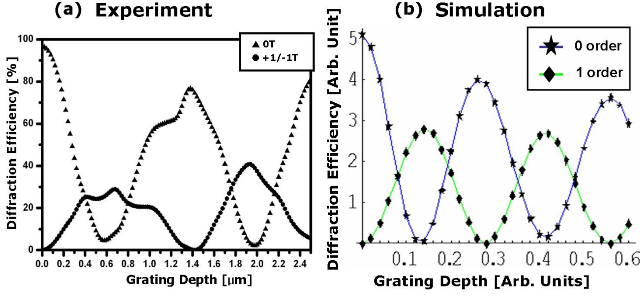

Fig. 3. Results of (a) experiment and (b) simulation for the TE diffraction efficiencies. '0 T' and '+1 / −1 T' in the graph legend of Figure (a) indicate '0 order' and '+1 order / −1 order', respectively.

$$S_{00}^{0,n+1} = \left[N_{00}^{n,n+1} - \left(D^{n,n+1}\right)^{-1} S_{01}^{0,n} \left(D^{n,n+1}\right)^{-1} N_{10}^{n,n+1}\right]^{-1} \times \left(D^{n,n+1}\right)^{-1} S_{00}^{0,n}, \quad (17)$$

$$S_{01}^{0,n+1} = \left[N_{00}^{n,n+1} - \left(D^{n,n+1}\right)^{-1} S_{01}^{0,n} \left(D^{n,n+1}\right)^{-1} N_{10}^{n,n+1}\right]^{-1} \times \left[\left(D^{n,n+1}\right)^{-1} S_{01}^{0,n} \left(D^{n,n+1}\right)^{-1} N_{11}^{n,n+1} - N_{01}^{n,n+1}\right], \quad (18)$$

$$S_{10}^{0,n+1} = S_{11}^{0,n} \left(D^{n,n+1}\right)^{-1} N_{10}^{n,n+1} S_{01}^{0,n+1} + S_{10}^{0,n}, \quad (19)$$

$$S_{11}^{0,n+1} = S_{11}^{0,n} \left(D^{n,n+1}\right)^{-1} N_{10}^{n,n+1} S_{01}^{0,n+1} + S_{10}^{0,n} \left(D^{n,n+1}\right)^{-1} N_{11}^{n,n+1}. \quad (20)$$

For a sack of thin films with L layers, this algorithm is started with $S(0,0) = I$, where I is a 2 by 2 identity matrix and is finished with $S(0, L+1)$. The amplitude coefficients of reflection ($\Re$) and transmission ($\Im$) are now given by

$$\Re = \frac{c_0^{(-)}}{c_0^{(+)}} = S_{10}^{0,L+1}, \Im = \frac{c_{L+1}^{(+)}}{c_0^{(+)}} = S_{00}^{0,L+1}. \quad (21)$$

IV. COMPARISON WITH EXPERIMETNAL RESULTS

Figure 3 shows the experimental and the simulated results of TE diffraction efficiencies. Both the experimental and the simulation conditions are a wavelength of 532-nm, an incident angle 0°, a pitch of 1025-nm and a substrate of fused silica with a refractive index of 1.46. The simulation results of Figure 3(b) show a good match with the experimental results of Figure 3(a) [6]. For two periods of TE diffraction of 0 / 1 order, the simulation

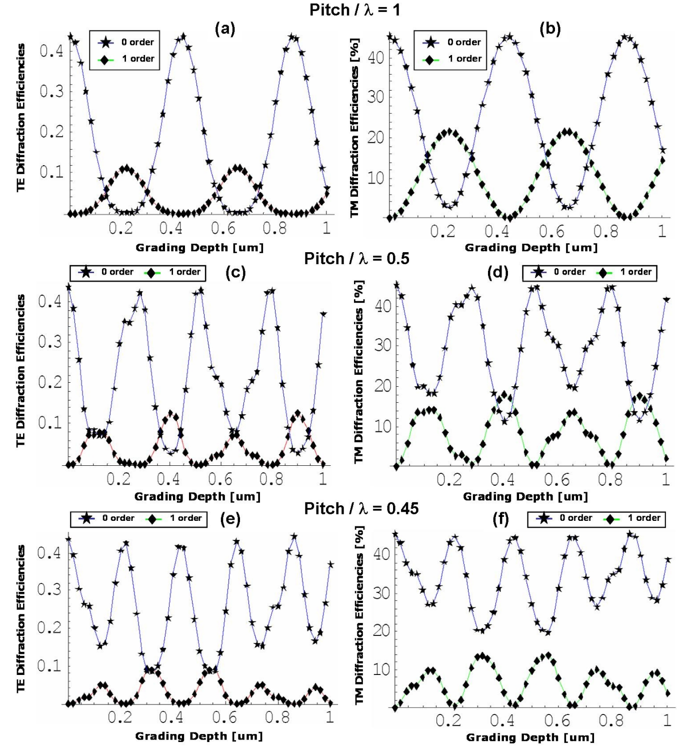

Fig. 4. Simulated diffraction efficiencies of (a) TE and (b) TM polarizations with pitch (p) / wavelength (λ) = 1, (c) TE and (d) TM polarizations with $p/\lambda = 0.5$ and (e) TE and (f) TM polarizations with $p/\lambda = 0.45$ by using the directed solution of Eqs. (10)−(14).

results within the grating depth of 0.51 arbitrary units corresponds to the experimental results within a 2.4-μm grating depth. For the diffraction efficiency, one arbitrary unit in Figure 3(b) corresponds to 20 % in Figure 3(a). Hence, we are confident that the simulation results within a proper range can describe the experimental physical and optical phenomena.

V. ANALYSIS

Figure 4 shows the simulated diffraction efficiencies of the TE and the TM modes by using the directed solution of Eqs. (10)−(14). For the diffracted orders of the TE and the TM modes, the diffraction efficiencies of the grating depths are calculated in terms of the ratio of the pitch to the wavelength. For simulation conditions, wavelength is 193-nm, incident angle is 0° and the refractive indices of regions 1 and 3 in Figure 1(b) are 1.0 and 2.0, respectively. When this pitch ratio is smaller than 1, the TE polarizations of Figures 4(c) and (e) become different with the TM polarizations of Figures 4(d) and (f) and the diffraction efficiencies of the diffracted orders become small. The separation of the diffracted orders in the TE and the TM modes means unstableness in this

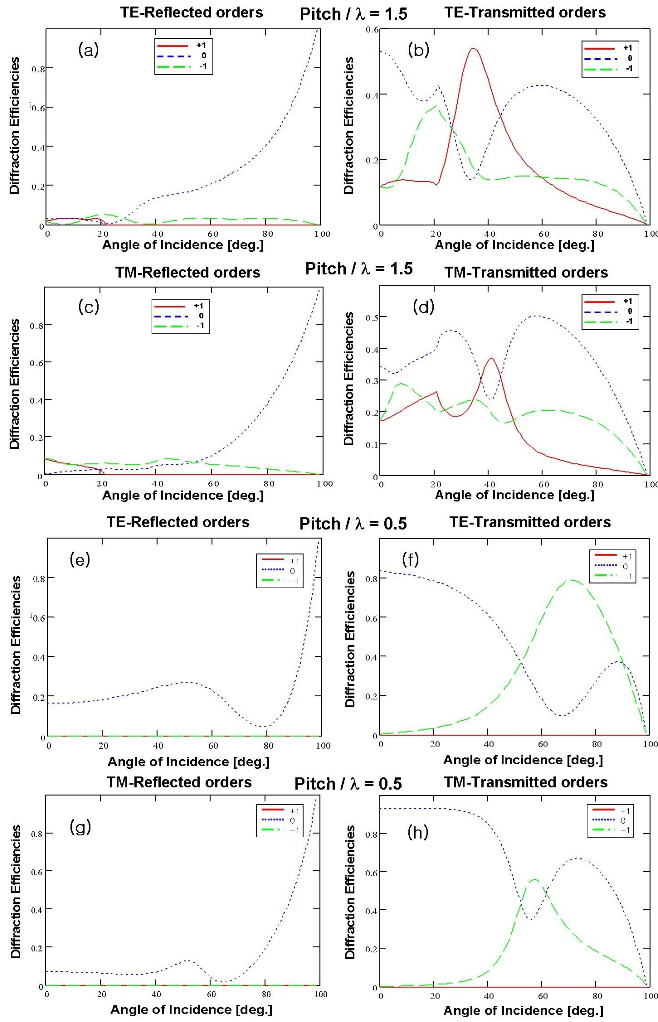

Fig. 5. Simulated diffraction efficiencies of pitch (p) / wavelength (λ) = 1.5 in (a) TE-reflected orders, (b) TE-transmitted orders, (c) TM-reflected orders and (d) TM-transmitted orders and of p/λ = 0.5 in (e) TE-reflected orders, (f) TE-transmitted orders, (g) TM-reflected orders and (h) TM-transmitted orders by using the scattering matrix of Eqs. (15)−(21). '+1', '0' and '−1' in the graph legends indicate '+1 order', '0 order' and '−1 order', respectively.

program. This unstableness is severe when the pitch is smaller than the wavelength. When the two diffracted orders form patterns, the diffracted orders of Figures 4 (a) and (b) with pitch / wavelength = 1 can make easily patterns in comparison with the diffracted orders of Figures 4(e) and (f) with pitch / wavelength = 0.45.

Figure 5 shows the simulation results for the diffraction efficiencies obtained by using the scattering matrix of Eqs. (15)−(21). For the diffracted orders of the TE and the TM modes, the diffraction efficiencies of the incidence angles are calculated in terms of the ratio of the pitch to the wavelength. The simulation conditions are the same as those of Figure 4. For the reflected and the transmitted orders, the diffraction efficiencies of the TE

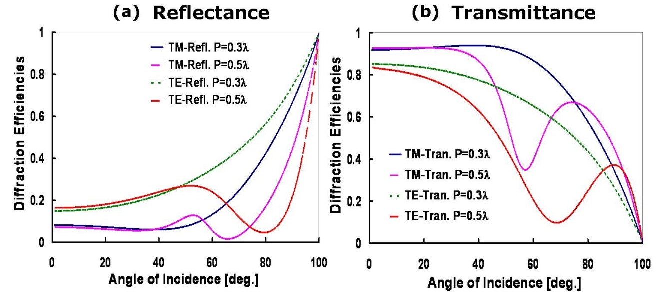

Fig. 6. Simulated results of diffraction efficiencies for various incident angle in (a) reflectance of the TE and the TM modes and (b) transmittance of the TE and the TM modes at the 0 order. 'TM-Refl. P = 0.3 λ' and 'TM-Tran. P = 0.3 λ' in the graph legends indicate 'TM-reflected zero order at a 0.3 ratio of pitch to incident wavelength' and 'TM-transmitted zero order at a 0.3 ratio of pitch to incident wavelength', respectively.

mode in Figures 5(a), (b), (e) and (f) are different with those of the TM mode in Figures 5(c), (d), (g) and (h). When the ratio of the pitch to the wavelength is small, the TE and the TM polarizations with the nonspecular (+1 and −1 orders) harmonics are small in comparison to those with the specular (0 order) harmonic and a variance of the TE and the TM polarizations is produced [4, 8].

Figure 6 shows the simulation results of diffraction efficiencies according to incident angle in the reflectance and the transmittance of the TE and the TM modes at the 0 order with the same simulation conditions as in Figure 5. According to simulation results, when the pitch is smaller than the incident wavelength, the variation of the diffraction efficiency with the 0 order is decreased. For transmittance under a 60° incident angle, the diffraction efficiency of the TM mode is larger than that of the TE mode, but for the reflectance, diffraction efficiency of the TM mode is smaller than that of the TE mode.

Due to the reduction in the ratio of the pitch to the wavelength, the diffraction variance of the TE and the TM polarizations degrade the resolution of the pattern formation. The optimized selection of the grating depths in Figure 4 and the incident angles in Figures 5 and 6 can reduce those unwanted effects.

VI. CONCLUSION

When the mask pattern is smaller than the wavelength in proximity and contact lithography, the diffraction effects of the TE and the TM polarizations are severe. For these physical and optical phenomena, an analytical model and two methods of the rigorous coupled-wave analysis (RCWA) are to calculate the diffraction efficiencies according to grating depths and incident angles. When the ratio of the pitch to the wavelength is

small at the 0° incident angle, the contribution of non-specular (+1 and −1 orders) harmonics to the TE and the TM polarizations is small in comparison to the specular (0 order) harmonics contribution and a variance of the TE and the TM polarizations is produced. For the transmittance under a 60° incident angle, the diffraction efficiency of the TM mode is larger than that of the TE mode, but for the reflectance, the diffraction efficiency of the TM mode is smaller than that of the TE mode. The effects of diffraction orders and the variance of the TE and the TM polarizations degrade the resolution of the pattern formation.

ACKNOWLEDGMENTS

This research was supported by the MIC(Ministry of Information and Communication), Korea, under the ITRC(Information Technology Research Center) support program supervised by the IITA(Institute of Information Technology Advancement) (IITA-2008-C109008010030).

REFERENCES

[1] S.-K. Kim and T. S. Kim, J. Korean Phys. Soc. **48**, 1661 (2006).
[2] S.-K. Kim and H.-K. Oh, J. Korean Phys. Soc. **47**, S377 (2005).
[3] Y. Hirai, Y. Inamto, K. Sugano, T. Tsuchiay and O. Tabata, J. Micromech. Microeng. **17**, 199 (2007).
[4] N. Chateau and J.-P. Hugonin, J. Opt. Soc. Am. **11**, 1321 (1994).
[5] F. Wang, M. K. Horn and A. Lakhtakia, Microelec. Eng. **71**, 34 (2004).
[6] Jae Wook Jeong, Master thesis, Seoul National University, 2005.
[7] A. G. Lopez and H. G. Craighead, Opt. Lett. **23**, 1627 (1998).
[8] S.-K. Kim, J. Korean Phys. Soc. **50**, 1952 (2007).